5-1-2002

Measurement of *B*-meson lifetimes using fully reconstructed B decays produced

Darin Acosta
University of Florida, acosta@phys.ufl.edu

Kenneth A. Bloom
University of Nebraska - Lincoln, kbloom2@unl.edu

Collider Detector at Fermilab Collaboration

Measurement of *B*-meson lifetimes using fully reconstructed *B* decays produced in $p\bar{p}$ collisions at $\sqrt{s}=1.8$ TeV

D. Acosta,[13] T. Affolder,[24] H. Akimoto,[47] M. G. Albrow,[12] D. Ambrose,[34] D. Amidei,[26] K. Anikeev,[25] J. Antos,[1] G. Apollinari,[12] T. Arisawa,[47] A. Artikov,[10] T. Asakawa,[45] W. Ashmanskas,[9] F. Azfar,[32] P. Azzi-Bacchetta,[33] N. Bacchetta,[33] H. Bachacou,[24] W. Badgett,[12] S. Bailey,[17] P. de Barbaro,[38] A. Barbaro-Galtieri,[24] V. E. Barnes,[37] B. A. Barnett,[20] S. Baroiant,[5] M. Barone,[14] G. Bauer,[25] F. Bedeschi,[35] S. Belforte,[44] W. H. Bell,[16] G. Bellettini,[35] J. Bellinger,[48] D. Benjamin,[11] J. Bensinger,[4] A. Beretvas,[12] J. P. Berge,[12] J. Berryhill,[9] A. Bhatti,[39] M. Binkley,[12] D. Bisello,[33] M. Bishai,[12] R. E. Blair,[2] C. Blocker,[4] K. Bloom,[26] B. Blumenfeld,[20] S. R. Blusk,[38] A. Bocci,[39] A. Bodek,[38] G. Bolla,[37] Y. Bonushkin,[6] D. Bortoletto,[37] J. Boudreau,[36] A. Brandl,[28] S. van den Brink,[20] C. Bromberg,[27] M. Brozovic,[11] E. Brubaker,[24] N. Bruner,[28] J. Budagov,[10] H. S. Budd,[38] K. Burkett,[17] G. Busetto,[33] A. Byon-Wagner,[12] K. L. Byrum,[2] S. Cabrera,[11] P. Calafiura,[24] M. Campbell,[26] W. Carithers,[24] J. Carlson,[26] D. Carlsmith,[48] W. Caskey,[5] A. Castro,[3] D. Cauz,[44] A. Cerri,[35] A. W. Chan,[1] P. S. Chang,[1] P. T. Chang,[1] J. Chapman,[26] C. Chen,[34] Y. C. Chen,[1] M.-T. Cheng,[1] M. Chertok,[5] G. Chiarelli,[35] I. Chirikov-Zorin,[10] G. Chlachidze,[10] F. Chlebana,[12] L. Christofek,[19] M. L. Chu,[1] J. Y. Chung,[30] W. -H. Chung,[48] Y. S. Chung,[38] C. I. Ciobanu,[30] A. G. Clark,[15] M. Coca,[38] A. P. Colijn,[12] A. Connolly,[24] M. Convery,[39] J. Conway,[40] M. Cordelli,[14] J. Cranshaw,[42] R. Culbertson,[12] D. Dagenhart,[46] S. D'Auria,[16] F. DeJongh,[12] S. Dell'Agnello,[14] M. Dell'Orso,[35] S. Demers,[38] L. Demortier,[39] M. Deninno,[3] P. F. Derwent,[12] T. Devlin,[40] J. R. Dittmann,[12] A. Dominguez,[24] S. Donati,[35] M. D'Onofrio,[35] T. Dorigo,[17] I. Dunietz,[12] N. Eddy,[19] K. Einsweiler,[24] J. E. Elias,[12] E. Engels, Jr.,[36] R. Erbacher,[12] D. Errede,[19] S. Errede,[19] Q. Fan,[38] H. -C. Fang,[24] R. G. Feild,[49] J. P. Fernandez,[37] C. Ferretti,[35] R. D. Field,[13] I. Fiori,[3] B. Flaugher,[12] G. W. Foster,[12] M. Franklin,[17] J. Freeman,[12] J. Friedman,[25] Y. Fukui,[23] I. Furic,[25] S. Galeotti,[35] A. Gallas,[29] M. Gallinaro,[39] T. Gao,[34] M. Garcia-Sciveres,[24] A. F. Garfinkel,[37] P. Gatti,[33] C. Gay,[49] D. W. Gerdes,[26] E. Gerstein,[8] P. Giannetti,[35] K. Giolo,[37] M. Giordani,[5] P. Giromini,[14] V. Glagolev,[10] D. Glenzinski,[12] M. Gold,[28] J. Goldstein,[12] I. Gorelov,[28] A. T. Goshaw,[11] Y. Gotra,[36] K. Goulianos,[39] C. Green,[37] G. Grim,[5] P. Gris,[12] C. Grosso-Pilcher,[9] M. Guenther,[37] G. Guillian,[26] J. Guimaraes da Costa,[17] R. M. Haas,[13] C. Haber,[24] S. R. Hahn,[12] C. Hall,[17] T. Handa,[18] R. Handler,[48] F. Happacher,[14] K. Hara,[45] A. D. Hardman,[37] R. M. Harris,[12] F. Hartmann,[21] K. Hatakeyama,[39] J. Hauser,[6] J. Heinrich,[34] A. Heiss,[21] M. Herndon,[20] C. Hill,[5] A. Hocker,[38] K. D. Hoffman,[9] R. Hollebeek,[34] L. Holloway,[19] B. T. Huffman,[32] R. Hughes,[30] J. Huston,[27] J. Huth,[17] H. Ikeda,[45] J. Incandela,[12,*] G. Introzzi,[35] A. Ivanov,[38] J. Iwai,[47] Y. Iwata,[18] E. James,[26] M. Jones,[34] U. Joshi,[12] H. Kambara,[15] T. Kamon,[41] T. Kaneko,[45] M. Karagoz Unel,[29] K. Karr,[46] S. Kartal,[12] H. Kasha,[49] Y. Kato,[31] T. A. Keaffaber,[37] K. Kelley,[25] M. Kelly,[26] R. D. Kennedy,[12] R. Kephart,[12] D. Khazins,[11] T. Kikuchi,[45] B. Kilminster,[38] B. J. Kim,[22] D. H. Kim,[22] H. S. Kim,[19] M. J. Kim,[8] S. B. Kim,[22] S. H. Kim,[45] Y. K. Kim,[24] M. Kirby,[11] M. Kirk,[4] L. Kirsch,[4] S. Klimenko,[13] P. Koehn,[30] K. Kondo,[47] J. Konigsberg,[13] A. Korn,[25] A. Korytov,[13] E. Kovacs,[2] J. Kroll,[34] M. Kruse,[11] V. Krutelyov,[41] S. E. Kuhlmann,[2] K. Kurino,[18] T. Kuwabara,[45] A. T. Laasanen,[37] N. Lai,[9] S. Lami,[39] S. Lammel,[12] J. Lancaster,[11] M. Lancaster,[24] R. Lander,[5] A. Lath,[40] G. Latino,[28] T. LeCompte,[2] K. Lee,[42] S. W. Lee,[41] S. Leone,[35] J. D. Lewis,[12] M. Lindgren,[6] T. M. Liss,[19] J. B. Liu,[38] T. Liu,[12] Y. C. Liu,[1] D. O. Litvintsev,[12] O. Lobban,[42] N. S. Lockyer,[34] J. Loken,[32] M. Loreti,[33] D. Lucchesi,[33] P. Lukens,[12] S. Lusin,[48] L. Lyons,[32] J. Lys,[24] R. Madrak,[17] K. Maeshima,[12] P. Maksimovic,[17] L. Malferrari,[3] M. Mangano,[35] G. Manca,[32] M. Mariotti,[33] G. Martignon,[33] A. Martin,[49] V. Martin,[29] J. A. J. Matthews,[28] P. Mazzanti,[3] K. S. McFarland,[38] P. McIntyre,[41] M. Menguzzato,[33] A. Menzione,[35] P. Merkel,[12] C. Mesropian,[39] A. Meyer,[12] T. Miao,[12] R. Miller,[27] J. S. Miller,[26] H. Minato,[45] S. Miscetti,[14] M. Mishina,[23] G. Mitselmakher,[13] Y. Miyazaki,[31] N. Moggi,[3] E. Moore,[28] R. Moore,[26] Y. Morita,[23] T. Moulik,[37] M. Mulhearn,[25] A. Mukherjee,[12] T. Muller,[21] A. Munar,[35] P. Murat,[12] S. Murgia,[27] J. Nachtman,[6] V. Nagaslaev,[42] S. Nahn,[49] H. Nakada,[45] I. Nakano,[18] C. Nelson,[12] T. Nelson,[12] C. Neu,[30] D. Neuberger,[21] C. Newman-Holmes,[12] C. -Y. P. Ngan,[25] H. Niu,[4] L. Nodulman,[2] A. Nomerotski,[13] S. H. Oh,[11] Y. D. Oh,[22] T. Ohmoto,[18] T. Ohsugi,[18] R. Oishi,[45] T. Okusawa,[31] J. Olsen,[48] W. Orejudos,[24] C. Pagliarone,[35] F. Palmonari,[35] R. Paoletti,[35] V. Papadimitriou,[42] D. Partos,[4] J. Patrick,[12] G. Pauletta,[44] M. Paulini,[8] C. Paus,[25] D. Pellett,[5] L. Pescara,[33] T. J. Phillips,[11] G. Piacentino,[35] K. T. Pitts,[19] A. Pompos,[37] L. Pondrom,[48] G. Pope,[36] T. Pratt,[32] F. Prokoshin,[10] J. Proudfoot,[2] F. Ptohos,[14] O. Pukhov,[10] G. Punzi,[35] A. Rakitine,[25] F. Ratnikov,[40] D. Reher,[24] A. Reichold,[32] P. Renton,[32] A. Ribon,[33] W. Riegler,[17] F. Rimondi,[3] L. Ristori,[35] M. Riveline,[43] W. J. Robertson,[11] T. Rodrigo,[7] S. Rolli,[46] L. Rosenson,[25] R. Roser,[12] R. Rossin,[33] C. Rott,[37] A. Roy,[37] A. Ruiz,[7] A. Safonov,[5] R. St. Denis,[16] W. K. Sakumoto,[38] D. Saltzberg,[6] C. Sanchez,[30] A. Sansoni,[14] L. Santi,[44] H. Sato,[45] P. Savard,[43] A. Savoy-Navarro,[12] P. Schlabach,[12] E. E. Schmidt,[12] M. P. Schmidt,[49] M. Schmitt,[29] L. Scodellaro,[33] A. Scott,[6] A. Scribano,[35] A. Sedov,[37] S. Segler,[12] S. Seidel,[28] Y. Seiya,[45] A. Semenov,[10] F. Semeria,[3] T. Shah,[25] M. D. Shapiro,[24] P. F. Shepard,[36] T. Shibayama,[45] M. Shimojima,[45] M. Shochet,[9] A. Sidoti,[33] J. Siegrist,[24] A. Sill,[42] P. Sinervo,[43] P. Singh,[19] A. J. Slaughter,[49] K. Sliwa,[46] C. Smith,[20] F. D. Snider,[12] A. Solodsky,[39] J. Spalding,[12] T. Speer,[15] M. Spezziga,[42] P. Sphicas,[25] F. Spinella,[35] M. Spiropulu,[9] L. Spiegel,[12] J. Steele,[48] A. Stefanini,[35] J. Strologas,[19] F. Strumia,[15] D. Stuart,[12] K. Sumorok,[25] T. Suzuki,[45] T. Takano,[31] R. Takashima,[18] K. Takikawa,[45] P. Tamburello,[11] M. Tanaka,[45] B. Tannenbaum,[6] M. Tecchio,[26] R. J. Tesarek,[12] P. K. Teng,[1] K. Terashi,[39] S. Tether,[25] A. S. Thompson,[16] E. Thomson,[30] R. Thurman-Keup,[2] P. Tipton,[38] S. Tkaczyk,[12] D. Toback,[41] K. Tollefson,[38] A. Tollestrup,[12] D. Tonelli,[35] M. Tonnesmann,[27] H. Toyoda,[31] W. Trischuk,[43] J. F. de Troconiz,[17] J. Tseng,[25] D. Tsybychev,[13] N. Turini,[35] F. Ukegawa,[45] T. Vaiciulis,[38] J. Valls,[40] E. Vataga,[35] S. Vejcik III,[12] G. Velev,[12] G. Veramendi,[24] R. Vidal,[12] I. Vila,[7]

R. Vilar,[7] I. Volobouev,[24] M. von der Mey,[6] D. Vucinic,[25] R. G. Wagner,[2] R. L. Wagner,[12] W. Wagner,[21] N. B. Wallace,[40] Z. Wan,[40] C. Wang,[11] M. J. Wang,[1] S. M. Wang,[13] B. Ward,[16] S. Waschke,[16] T. Watanabe,[45] D. Waters,[32] T. Watts,[40] M. Weber,[24] H. Wenzel,[21] W. C. Wester III,[12] A. B. Wicklund,[2] E. Wicklund,[12] T. Wilkes,[5] H. H. Williams,[34] P. Wilson,[12] B. L. Winer,[30] D. Winn,[26] S. Wolbers,[12] D. Wolinski,[26] J. Wolinski,[27] S. Wolinski,[26] S. Worm,[40] X. Wu,[15] J. Wyss,[35] U. K. Yang,[9] W. Yao,[24] G. P. Yeh,[12] P. Yeh,[1] J. Yoh,[12] C. Yosef,[27] T. Yoshida,[31] I. Yu,[22] S. Yu,[34] Z. Yu,[49] J. C. Yun,[12] A. Zanetti,[44] F. Zetti,[24] and S. Zucchelli[3]

(CDF Collaboration)

[1]*Institute of Physics, Academia Sinica, Taipei, Taiwan 11529, Republic of China*
[2]*Argonne National Laboratory, Argonne, Illinois 60439*
[3]*Istituto Nazionale di Fisica Nucleare, University of Bologna, I-40127 Bologna, Italy*
[4]*Brandeis University, Waltham, Massachusetts 02254*
[5]*University of California at Davis, Davis, California 95616*
[6]*University of California at Los Angeles, Los Angeles, California 90024*
[7]*Instituto de Fisica de Cantabria, CSIC–University of Cantabria, 39005 Santander, Spain*
[8]*Carnegie Mellon University, Pittsburgh, Pennyslvania 15218*
[9]*Enrico Fermi Institute, University of Chicago, Chicago, Illinois 60637*
[10]*Joint Institute for Nuclear Research, RU-141980 Dubna, Russia*
[11]*Duke University, Durham, North Carolina 27708*
[12]*Fermi National Accelerator Laboratory, Batavia, Illinois 60510*
[13]*University of Florida, Gainesville, Florida 32611*
[14]*Laboratori Nazionali di Frascati, Istituto Nazionale di Fisica Nucleare, I-00044 Frascati, Italy*
[15]*University of Geneva, CH-1211 Geneva 4, Switzerland*
[16]*Glasgow University, Glasgow G 12 8QQ, United Kingdom*
[17]*Harvard University, Cambridge, Massachusetts 02138*
[18]*Hiroshima University, Higashi-Hiroshima 724, Japan*
[19]*University of Illinois, Urbana, Illinois 61801*
[20]*The Johns Hopkins University, Baltimore, Maryland 21218*
[21]*Institut für Experimentelle Kernphysik, Universität Karlsruhe, 76128 Karlsruhe, Germany*
[22]*Center for High Energy Physics, Kyungpook National University, Taegu 702-701, Korea,*
Seoul National University, Seoul 151-742, Korea,
and SungKyunKwan University, Suwon 440-746, Korea
[23]*High Energy Accelerator Research Organization (KEK), Tsukuba, Ibaraki 305, Japan*
[24]*Ernest Orlando Lawrence Berkeley National Laboratory, Berkeley, California 94720*
[25]*Massachusetts Institute of Technology, Cambridge, Massachusetts 02139*
[26]*University of Michigan, Ann Arbor, Michigan 48109*
[27]*Michigan State University, East Lansing, Michigan 48824*
[28]*University of New Mexico, Albuquerque, New Mexico 87131*
[29]*Northwestern University, Evanston, Illinois 60208*
[30]*The Ohio State University, Columbus, Ohio 43210*
[31]*Osaka City University, Osaka 588, Japan*
[32]*University of Oxford, Oxford OX 1 3RH, United Kingdom*
[33]*Universita di Padova, Istituto Nazionale di Fisica Nucleare, Sezione di Padova, I-35131 Padova, Italy*
[34]*University of Pennsylvania, Philadelphia, Pennsylvania 19104*
[35]*Istituto Nazionale di Fisica Nucleare, University and Scuola Normale Superiore of Pisa, I-56100 Pisa, Italy*
[36]*University of Pittsburgh, Pittsburgh, Pennsylvania 15260*
[37]*Purdue University, West Lafayette, Indiana 47907*
[38]*University of Rochester, Rochester, New York 14627*
[39]*Rockefeller University, New York, New York 10021*
[40]*Rutgers University, Piscataway, New Jersey 08855*
[41]*Texas A&M University, College Station, Texas 77843*
[42]*Texas Tech University, Lubbock, Texas 79409*
[43]*Institute of Particle Physics, University of Toronto, Toronto M 5S 1A 7, Canada*
[44]*Istituto Nazionale di Fisica Nucleare, University of Trieste/Udine, Italy*
[45]*University of Tsukuba, Tsukuba, Ibaraki 305, Japan*
[46]*Tufts University, Medford, Massachusetts 02155*
[47]*Waseda University, Tokyo 169, Japan*
[48]*University of Wisconsin, Madison, Wisconsin 53706*
[49]*Yale University, New Haven, Connecticut 06520*

(Received 13 March 2002; published 20 May 2002)

We present an improved measurement of *b*-meson lifetimes using fully reconstructed *B*-decays produced in $p\bar{p}$ collisions at $\sqrt{s}=1.8$ TeV, using 114 pb^{-1} of data collected at the Collider Detector at Fermilab. We obtain $\tau(B^+)=1.636\pm0.058(\mathrm{stat})\pm0.025(\mathrm{syst})$ ps, $\tau(B^0)=1.497\pm0.073(\mathrm{stat})\pm0.032(\mathrm{syst})$ ps and for the lifetime ratio $\tau(B^+)/\tau(B^0)=1.093\pm0.066(\mathrm{stat})\pm0.028(\mathrm{syst})$.

DOI: 10.1103/PhysRevD.65.092009 PACS number(s): 14.40.Nd, 13.25.Hw

I. INTRODUCTION

Accurate measurements of *B* meson lifetimes are essential in measuring standard model parameters and related phenomena, for example in the accurate determination of the Cabibbo-Kobayashi-Maskawa (CKM) matrix element V_{cb}, and the measurement of the time dependence of B-$\bar{B}$ oscillations. To first order, meson lifetimes can be calculated by a procedure in which the lighter quark in the meson is neglected and the lifetime of the meson is determined by the heavier quark. In this so-called spectator model, all hadrons containing a *b* quark have the same lifetime. This model breaks down as the difference in mass of the light and heavy quarks bound in the meson becomes smaller and other corrections are considered. Several processes contribute corrections to the spectator model [1]; these include the *W* exchange process for the B^0, and the annihilation graph for the B^+ [2]. Other non-spectator corrections are caused by Pauli final state interference effects. Calculations using the spectator model and several corrections predict a ratio of lifetimes of 1.05–1.2 for the B^+ and B^0 mesons. This is smaller than the corresponding ratio of 2.5 for the D^+ and D^0 lifetimes [3] and is due to the relatively heavier *b* quark.

We report on the new measurement of the lifetimes of *B* mesons using fully reconstructed decays of B^+ and B^0 with J/ψ and $\psi(2S)$ final states. The results reported here supersede the results of our previous measurement reported in [4]. Compared to our previous measurement we have used more data [5], a more refined fitting method, and for the first time we have included final states with $J/\psi\to e^+e^-$ and $\psi(2S)\to\mu^+\mu^-$.

II. THE CDF DETECTOR

In the following section we describe the Collider Detector at Fermilab (CDF) [6], starting with the tracking system which is immersed in a 1.4 T solenoidal magnetic field. The innermost tracking device is a silicon micro-strip vertex detector (SVX) [7] that provides spatial measurements in the r-ϕ [8] plane with an impact parameter resolution of $\sigma_D(p_T)=(13+40/p_T)$ μm where p_T is the transverse momentum of the track in units of GeV/c [9]. The SVX is followed by a set of time projection chambers (VTX) which measures the position of the proton-antiproton interaction (the primary vertex) along the beam line. Surrounding the VTX is the central tracking chamber (CTC), a 3 m long cylindrical drift chamber from 0.3 to 1.3 m in radius covering the pseudo-rapidity interval $|\eta|<1.0$. The CTC contains 84 layers of sense wires, grouped into nine alternating axial and stereo superlayers providing three-dimensional tracking. The outer 54 layers of the CTC are instrumented to record the specific ionization $\mathrm{d}E/\mathrm{d}x$ of charged particles.

Outside the solenoid are central electromagnetic (CEM) and hadronic (CHA) calorimeters ($|\eta|<1.1$) with a segmentation of $\Delta\eta\times\Delta\varphi\sim0.1\times15°$. The energy resolution of the central calorimeter is $\sigma(E_T)/E_T=[(13.5\%/\sqrt{E_T})^2+(2\%)^2]^{1/2}$ for electromagnetic showers where E_T is the transverse energy measured in GeV. A layer of proportional chambers (CES) with wire and strip readout, is located six radiation lengths deep in the CEM calorimeter approximately near shower maximum for electromagnetic showers. The CES provides a measurement of electromagnetic shower profiles in both the φ and z directions. Proportional chambers located between the solenoid and the CEM comprise the central pre-radiator detector (CPR) which samples the early development of electromagnetic showers in the material of the solenoid coil, providing position information in r-φ. The central muon system, consisting of three components, is capable of detecting muons with $p_T\geq1.4$ GeV/c in the pseudo-rapidity interval $|\eta|<1.0$. The CMU system covers the region $|\eta|<0.6$ and consists of 4 layers of planar drift chambers outside the hadron calorimeter allowing the reconstruction of track segments for charged particles penetrating the 5 absorption lengths of material. Outside the CMU there are 3 additional absorption lengths of steel followed by 4 layers of drift chambers (CMP). Finally, the CMX system extends the coverage up to pseudo-rapidity $|\eta|<1.0$. Depending on the incident angle, particles have to penetrate 6–9 absorption lengths of material to be detected in the CMX.

III. TRIGGER AND LEPTON SELECTION

CDF has a three level trigger system. The first two levels are implemented in hardware, while the third is a software trigger which is a version of the offline reconstruction software optimized for speed. For this measurement two types of triggers are relevant: the dimuon [12] and the single electron triggers. No dielectron trigger was available.

For the dimuons the level 1 triggers require two track segments in the muon chambers. At level 2, tracks found in the CTC by the central fast track processor (CFT) [10] are associated with track segments in the muon chambers. Two different p_T thresholds at approximately 2 and 2.5 GeV/c are used in our trigger, depending on whether one or both muons are required to be found in the CFT. The level 3

*Present address: University of California, Santa Barbara, CA 93106.

trigger requires two muon candidates after full reconstruction. The following muon selection criteria are applied: the separation between the track in the muon chamber and the extrapolated CTC track is calculated in both the transverse and longitudinal planes. In each view, the difference is required to be less than 3.0 standard deviations (σ) from zero, where σ is the sum in quadrature of the multiple scattering and measurement uncertainties. The energy deposited in the hadronic calorimeter by each muon is required to be greater than 0.1 GeV [11].

The single electron trigger requires electromagnetic energy deposition in the CEM at level 1 and a matching CFT track at level 2. The efficiency of finding an electron at level 1 rises from 15% at $E_T(e)=5$ GeV to 90% for $E_T(e)>6.5$ GeV. The level 3 trigger requires an electron candidate after full reconstruction. We distinguish between the electrons which fired the trigger and "soft" electrons not necessarily found by the standard electron reconstruction which does not identify electrons below $E_T(e)=5$ GeV. The trigger electrons are identified by requiring that the longitudinal shower profile is consistent with an electron shower. The lateral shower profiles as measured with the CEM and CES are required to be consistent with test beam data. To identify "soft" electrons a special algorithm was used which requires a good match between the extrapolated CTC tracks and the CES strip and wire clusters; the ratio of the energy deposited in the electromagnetic and the hadronic compartment of the calorimeter is required to be $\mathrm{E}_{Had}/\mathrm{E}_{EM}<0.125$. The ionization loss in the CTC has to be consistent with that of an electron and a minimum charge deposition in the CPR corresponding to several minimum ionizing particles is required.

IV. CANDIDATE SELECTION

In this section we describe the selection criteria for fully reconstructed B^+ and B^0 meson candidates. The four charmonium decay modes used in this study are $J/\psi\to\mu^+\mu^-$, $J/\psi\to e^+e^-$, $\psi(2S)\to\mu^+\mu^-$ and $\psi(2S)\to J/\psi\ \pi^+\pi^-\to\mu^+\mu^-\pi^+\pi^-$. B^+ mesons are reconstructed in the decay modes $J/\psi K^+$, $J/\psi K^{*+}$, $\psi(2S)K^+$, and $\psi(2S)K^{*+}$, while B^0 mesons are reconstructed in the decay modes $J/\psi K_S^0$ and $J/\psi K^{*0}$. The kaons are reconstructed using the decay channels $K^{*0}\to K^+\pi^-$, $K^{*+}\to K_S^0\pi^+$, and $K_S^0\to\pi^+\pi^-$. K^{*0} candidates are accepted if their invariant $K\pi$ mass is within ± 80 MeV/c^2 of the world average K^{*0} mass [3]. Since swapping the assignment of the kaon and pion masses for the two tracks forming a K^{*0} candidate can also result in a K^{*0} candidate within the ± 80 MeV/c^2 mass window, the K^{*0} combination closest to the world average mass value is chosen. Minimum transverse momentum (P_T) thresholds for the B meson and the kaons affect the signal-to-noise (S/N) ratio. They are chosen individually for each decay channel for minimal statistical uncertainty of the fitted lifetime. P_T thresholds for the B mesons vary between 4.5 and 5.5 GeV/c; for the kaons, we use thresholds between 0.75 and 1.25 GeV/c. To ensure well measured B decay vertices we require each track to be measured with several hits in at least 2 out of 5 axial superlayers and at least 2 out of 4 stereo

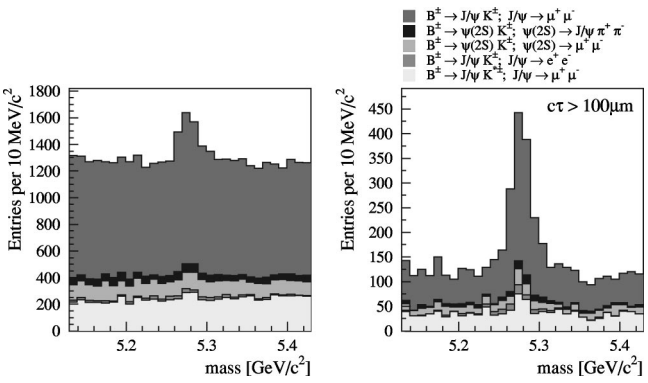

FIG. 1. The mass distribution for B^+ candidates (left). For the right histogram, a cut $c\tau>100$ μm is applied to illustrate the low background mass distribution for higher lifetime. The cut is not used in the analysis.

superlayers of the CTC. The two leptons originating from the J/ψ or $\psi(2S)$ decay are required to be measured in at least 3 out of the 4 layers of the SVX, resulting in a sample of $\approx 6000\ J/\psi\to e^+e^-$, $\approx 7800\ \psi(2S)\to\mu^+\mu^-$, $\approx 3500\ \psi(2S)\to J/\psi\pi^+\pi^-$ and $\approx 260000\ J/\psi\to\mu^+\mu^-$ candidates. For all other tracks SVX information is used if available.

In the case of B decays into $J/\psi\to e^+e^-$ final states, the bremsstrahlung losses of the electrons cause a smaller measured transverse momentum of the J/ψ and lead to a low mass tail in the dielectron invariant mass spectrum. The reconstructed values of the invariant mass and transverse momentum of the B meson would be lower than the true values. The reconstructed B mass is corrected by adding the difference of the true and reconstructed J/ψ masses. The necessary correction to the reconstructed B transverse momentum $[P_T(B)]$ due to bremsstrahlung is estimated using Monte Carlo generated data, including a full simulation of the CDF detector which includes the correct description of the mass distribution in the detector. The relative difference (loss) $([P_T(\mathrm{true})-P_T(\mathrm{measured})]/P_T(\mathrm{true}))$ as a function of the dielectron mass can be parametrized with sufficient accuracy by a straight line. The correction varies from 3.5% to 1.0% for dielectron mass values varying from 2.9 to 3.05 GeV/c^2. This correction is applied to all events with a dielectron in-

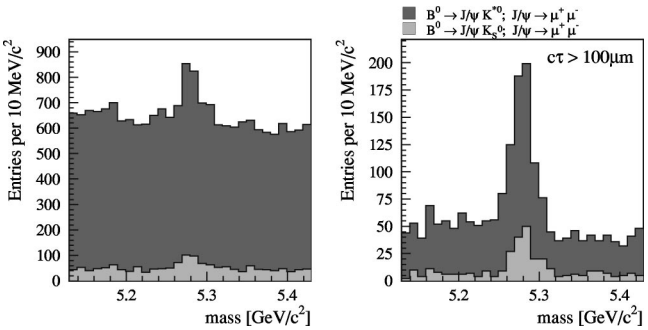

FIG. 2. The mass distribution for B^0 candidates (left). For the right histogram, a cut $c\tau>100$ μm is applied to illustrate the low background mass distribution for higher lifetime. The cut is not used in the analysis.

TABLE I. The number of fitted candidate events, measured lifetimes and corresponding statistical uncertainties for the individual five B^+ and two B^0 decay channels.

B^+ decay channels	# of candidates	Fitted lifetime (ps)
$J/\psi K^{\pm}$; $J/\psi \to \mu^+\mu^-$	906±37	1.653±0.061
$J/\psi K^{\pm}$; $J/\psi \to e^+e^-$	85±10	1.745±0.210
$\psi(2S)K^{\pm}$; $\psi(2S) \to \mu^+\mu^-$	57±11	1.404±0.249
$\psi(2S)K^{\pm}$; $\psi(2S) \to J/\psi\pi^+\pi^-$	49±10	1.504±0.256
$J/\psi K^{*\pm}$; $K^{*\pm} \to K^0_S\pi^{\pm}$	86±13	1.596±0.234

B^0 decay channels	# of candidates	Fitted lifetime (ps)
$J/\psi K^0_S$; $K^0_S \to \pi^+\pi^-$	135±14	1.373±0.137
$J/\psi K^{*0}$; $K^{*0} \to K^{\pm}\pi^{\mp}$	430±26	1.548±0.083

variant mass smaller than 3.057 GeV/c^2. Figures 1 and 2 show the reconstructed invariant mass distributions for B^+ and B^0 candidates, respectively. The different gray scales indicate the contributions of the different selections. We achieve a mass resolution of typically 13 MeV/c^2 for signal candidates.

V. THE PROPER DECAY LENGTH $c\tau$

The vertex and mass constrained J/ψ and $\psi(2S)$ candidates together with the K^+, K^{*+}, K^0_S or K^{*0} candidates are fit to a common vertex, yielding the two-dimensional B meson decay length L^B_{xy} defined as

$$L^B_{xy} = \frac{\vec{X}\cdot\vec{P}^B_T}{|\vec{P}^B_T|}, \tag{1}$$

where $\vec{P}^B_T$ is the transverse B momentum vector and $\vec{X}$ is the vector pointing from the primary vertex to the B decay vertex. We use the average beam position as an estimate of the primary vertex. This was calculated offline for each data acquisition run. Typically the transverse intensity profile of the beam was roughly circular and could be approximated by a Gaussian with $\sigma \approx 25$ μm [4]. We define the proper decay length (proper decay time scaled by the speed of light c) as $c\tau = L_{xy}\cdot m_B/P^B_T$ where P^B_T is the measured transverse momentum and m_B is the world average mass [3] of the B hadron. The average uncertainty on $c\tau$ is ≈ 40 μm.

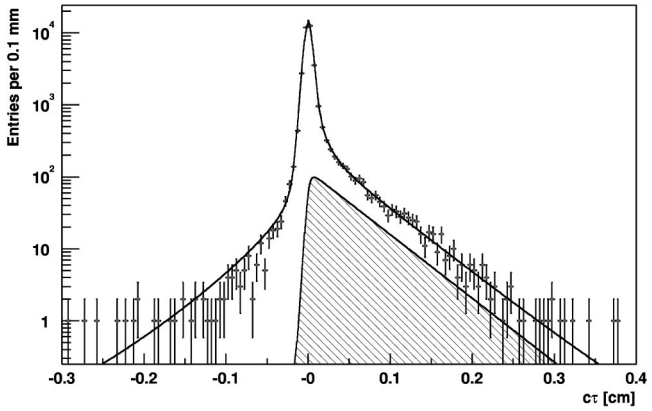

FIG. 3. The proper decay length ($c\tau$) distribution of all B^+ decay channels combined with the fitted function superimposed. The hatched area is the signal contribution.

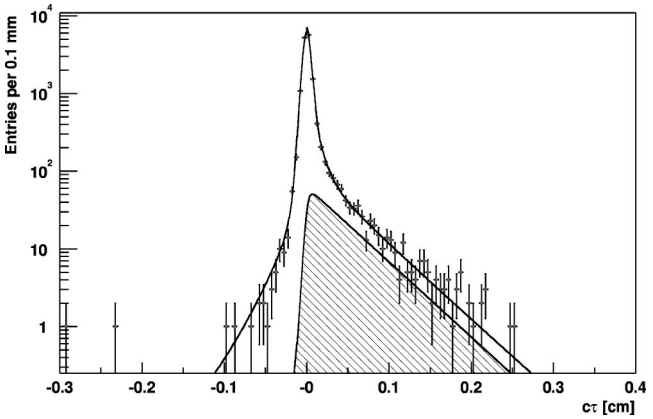

FIG. 4. The proper decay length ($c\tau$) distribution of all B^0 decay channels combined with the fitted function superimposed. The hatched area is the signal contribution.

VI. THE FITTING PROCEDURE

To extract the average lifetimes from the data, the mass and lifetime distributions are fit simultaneously using an unbinned logarithmic-likelihood method. The logarithmic-likelihood function to be minimized in this combined fit has the following form:

$$\mathcal{L} = -2\sum_{i=1}^{K}\sum_{j=1}^{N_i}\log P. \tag{2}$$

K is the number of data samples (decay channels). N_i is the number of events in data sample i. The normalized bivariate probability density function P depends on the mass and proper decay length distributions:

$$P(c\tau_j, m_j|\sigma^j_{c\tau}, \sigma^j_m) = (1-f_B)\cdot F_{sig}(c\tau_j|\sigma^j_{c\tau})\cdot M_{sig}(m_j|\sigma^j_m) + f_B\cdot F_{bgr}(c\tau_j|\sigma^j_{c\tau})\cdot M_{bgr}(m_j|\sigma^j_m)$$

TABLE II. Summary of the systematic uncertainties.

Description	Contribution B^+	Contribution B^0
Background parametrizations	4 μm	4 μm
Non-Gaussian tails	6 μm	8.5 μm
Fitting procedure bias	1 μm	1 μm
Residual misalignment of the SVX	1.5 μm	1.5 μm
Total systematic uncertainty	7.4 μm	9.6 μm
	0.025 ps	0.032 ps

where f_B is the background fraction, $c\tau_j$ is the measurement of the proper decay length, $\sigma^j_{c\tau}$ is the calculated uncertainty of $c\tau_j$, m_j is the measurement of the invariant mass, and σ^j_m is the calculated uncertainty of the invariant mass. P is normalized as

$$\int_{M_{min}}^{M_{max}} \int_{-\infty}^{\infty} P(c\tau, m | \sigma^j_{c\tau}, \sigma^j_m) d(c\tau) dm = 1, \qquad (3)$$

where M_{min} and M_{max} are the lower and upper bound of our signal mass window ± 150 MeV/c^2 around the world average B meson mass. The lifetime distribution of the signal (F_{sig}) is parametrized by an exponential function convoluted with a Gaussian function. We found that the lifetime distribution of the background (F_{bgr}) is well described by a central Gaussian and the sum of two exponential functions for the positive $c\tau$ region and one exponential function for the negative $c\tau$ region. To study the shape of the lifetime distribution of the background we used two sideband regions where the upper and lower sideband windows were each 0.1 GeV/c^2 wide and started at ± 0.050 GeV/c^2 from the world average value B mass of 5.279 GeV/c^2 [3]. The background events in the peak region were assumed to have the same proper decay length distribution as events in the sideband regions. The mass distributions of signal (M_{sig}) and background (M_{bgr}) are parametrized by a Gaussian function and a first order polynomial, respectively. To combine the results from all decay channels that measure either a B^0 or B^+ meson lifetime, we first fit for the lifetime in each channel as described. With this preliminary determination of the best fit lifetime, background shape and fraction complete, we combine all the channels and fit all the decay channels for either the B^0 or B^+. The only parameters common to all decay channels are the B meson lifetime and mass. The background shapes and fractions for each mode are parametrized and fit for separately.

Table I shows the number of contributed signal events as estimated by the fit and the lifetime results with their statistical uncertainties for the different decay channels. The results of the individual fits agree within statistical uncertainties. Figures 3 and 4 show the combined proper decay length distributions for charged and neutral B candidates, respectively.

VII. SYSTEMATIC UNCERTAINTIES

Table II summarizes all sources of systematic uncertainties that were considered. In order to determine an uncertainty due to the possible choice of different background parametrizations, the fractions and length scales of the three exponential functions are varied by ± 1 σ of the best fit values and fixed in the fit. In addition different parametrizations were used, e.g. only one exponential to describe the positive $c\tau$ region. Non-Gaussian contributions in the resolution function were studied by adding a wider Gaussian with σ fixed to 100 μm to the resolution function. Then we let the fraction of this second Gaussian float in the fit. A bias due to the fitting procedure itself was estimated by generating several hundred Monte Carlo samples and comparing the fit result with the true value. The bias due to misalignment changing the length scale of the SVX detector was studied in [4]. This bias cancels out in the lifetime ratio.

VIII. RESULTS

The results of the combined fit provides our measurement of the following quantities:

$$\tau(B^+) = (1.636 \pm 0.058 \pm 0.025)\,\text{ps},$$

$$\tau(B^0) = (1.497 \pm 0.073 \pm 0.032)\,\text{ps},$$

$$\tau(B^+)/\tau(B^0) = 1.093 \pm 0.066 \pm 0.028. \qquad (4)$$

This reduces the uncertainties compared to our previous results [4] by 19% and 13% for $\tau(B^+)$ and $\tau(B^0)$, respectively.

ACKNOWLEDGMENTS

We thank the Fermilab staff and the technical staffs of the participating institutions for their vital contributions. This work was supported by the U.S. Department of Energy and National Science Foundation; the Italian Istituto Nazionale di Fisica Nucleare; the Ministry of Education, Culture, Sports, Science, and Technology of Japan; the Natural Sciences and Engineering Research Council of Canada; the National Science Council of the Republic of China; the Swiss National Science Foundation; the A. P. Sloan Foundation; the Bundesministerium fuer Bildung und Forschung, Germany; the Korea Science and Engineering Foundation (KoSEF); the Korea Research Foundation; and the Comision Interministerial de Ciencia y Tecnologia, Spain.

[1] D. Becirevic, hep-ph/0110124; M.B. Voloshin, hep-ph/0004257; M. Neubert, hep-ph/9707217; I. Bigi, hep-ph/0001003.

[2] Throughout this paper charge conjugation symmetry is implied.

[3] Particle Data Group, D.E. Groom *et al.*, Eur. Phys. J. C **15**, 1 (2000); and 2001 off-year partial update for the 2002 edition available on the PDG WWW pages (URL: http://pdg.lbl.gov/).

[4] CDF Collaboration, F. Abe *et al.*, Phys. Rev. D **57**, 5382 (1998).

[5] The data sample of our previous analysis consisted of 106 pb^{-1} of $p\bar{p}$ collisions at $\sqrt{s} = 1.8$ TeV collected by the CDF detector at the Fermilab Tevatron collider during 1992–1995 (run 1). Of this, approximately 19.5 pb^{-1} were collected during the 1992–1993 running period (run 1A), and approximately 86.5 pb^{-1} were collected during the 1994–1995 run-

ning period (run 1B). In this analysis additional beam line information is used as well as 7.8 pb^{-1} of data from an additional running period (run 1C).

[6] CDF Collaboration, F. Abe *et al.*, Nucl. Instrum. Methods Phys. Res. A **271**, 387 (1988); Phys. Rev. D **50**, 2966 (1994).

[7] D. Amidei *et al.*, Nucl. Instrum. Methods Phys. Res. A **350**, 73 (1994).

[8] The polar angle (θ) in cylindrical coordinates is measured from the proton beam which defines the z axis, and the azimuthal angle (ϕ) from the plane of the Fermilab Tevatron. The pseudorapidity (η) is defined as $\eta = -\ln[\tan(\theta/2)]$. Throughout this paper ''transverse'' refers to the plane perpendicular to the proton beam and ''longitudinal'' refers to the axis parallel to the proton beam (z axis).

[9] The track impact parameter D is defined as the distance of closest approach, measured in the plane perpendicular to the beam, of the track helix to the beam axis.

[10] G. Foster *et al.*, Nucl. Instrum. Methods Phys. Res. A **269**, 93 (1988).

[11] The value of 0.1 GeV is several σ lower (based on the rms of the Landau distribution below the peak) than the average expected energy loss from a minimum ionizing particle.

[12] For a detailed description of the dimuon trigger, see CDF Collaboration, F. Abe *et al.*, Phys. Rev. D **57**, 3811 (1998). The analysis described there required events to come from a well defined trigger path. Here we also accepted volunteers, meaning events selected by a different trigger.